

Letter

Ferroelectric-to-relaxor crossover in Sb doped PLZT $x/52/48$ ($2 \leq x \leq 16$) piezoelectric ceramics

ARTICLE INFO

Keywords:

Dielectric behavior
Ferroelectrics
Phase transition
Relaxor

ABSTRACT

Dielectric behavior and diffuse phase transition have been investigated in Sb doped lead lanthanum zirconate titanate (PLZT) ceramics to understand the role of La and Sb in ferroelectric-to-relaxor crossover. Rayleigh and Curie–Weiss type law fittings show that the La substitution gradually transforms the PLZTs from ferroelectric to relaxor, while Sb dopants weaken the diffuseness and dielectric dispersion. Vogel–Fulcher model reveals that the samples at high La concentration are fully in relaxor state comparable to the undoped PLZTs.

Production and hosting by Elsevier B.V. on behalf of The Ceramic Society of Japan and the Korean Ceramic Society.

1. Introduction

Solid solution of $\text{Pb}_{1-x}\text{La}_x(\text{Zr}_y\text{Ti}_{1-y})_{1-x/4}\text{O}_3$ (PLZT) is the most investigated A-site substituted lead zirconate titanate (PZT) ferroelectric material for wide applications [1–6]. The La^{3+} substitution for Pb^{2+} of the PZTs introduces A-site vacancies, decreases oxygen vacancies, and reduces the domains to nano-size, inducing a gradual ferroelectric–relaxor transition. Polar relaxation like frequency dispersion is not featured in PZTs because of their normal, long-range ferroelectric order. However, when aliovalent cations, e.g. La^{3+} , are substituted into PZT body, random distributed vacancies hinder the onset of long-range order (LRO). These vacancies and composition fluctuations create local heterogeneous structures in the form of polar nano-regions (PNRs), which can transform into macroscopic domains with assistance of external electric field. At this point, a relaxor state is formed, featured with a slim electrical hysteresis loop that makes it a great candidate for capacitive energy storage application [4,6,7].

Although not all aliovalent cations can trigger the relaxor state in PZTs [4,5], some dopants, e.g. Sb^{5+} , can boost the piezoelectric activity of PZTs. Therefore, it is interesting to dope one or more element species along with the La^{3+} substitution to investigate the ferroelectric–relaxor transition in PLZTs. Several groups have already tried to co-dope La and other ions into PZTs. For example, Helke and Lubitz [8] and Rai and Sharma [9] tried to

co-dope La and Sb ions to modify the piezoelectric properties of PZT ceramics and investigate these ceramic's phase transitions. Pérez-Delfín et al. [10] studied the relaxor behavior in MnO_2 doped PLZT ceramics. However, to our knowledge, careful reports on the ferroelectric–relaxor transition of PLZT due to the introduction of aliovalent cation are still absent. In this letter, with a fixed amount of Sb_2O_5 (1.5 wt%) addition, the effect of La substitution for Pb on the ferroelectric-to-relaxor phase transition of PLZT $x/52/48$ ($2 \leq x \leq 16$, where x is the mole fraction) was investigated systematically, and the intrinsic mechanism was discussed.

2. Experimental procedure

All samples were prepared by the conventional solid-state reaction route. Raw materials of Pb_3O_4 , La_2O_3 , TiO_2 , ZrO_2 , and Sb_2O_5 were weighed carefully according to the chemical composition of $\text{Pb}_{1-x}\text{La}_x(\text{Zr}_{0.52}\text{Ti}_{0.48})_{1-x/4}\text{O}_3 + 1.5 \text{ wt\% } \text{Sb}_2\text{O}_5$ ($x = 0.02, 0.04, 0.06, 0.08, 0.10, 0.12, 0.14, 0.16$). 0.3 wt% excess Pb_3O_4 was added to compensate the lead loss during sintering at high temperature. The mixtures were ball-milled in distilled water for 2 h, and then dried and calcined in air at 900°C for 4 h. Subsequently, the ball-milled powders were pressed into cylindrical disks under a pressure of 25 MPa. After burning out the binder of paraffin wax at 760°C for 3.5 h, the green compacts were sealed in crucibles and sintered at 1250°C for 2 h. The as-prepared pellets were polished, and silver electrodes were screen-printed and fired at 800°C for 10 min. Finally, the samples with diameter of 12 mm and thickness of 1.5 mm were obtained. The crystalline structure was determined by an X-ray diffractometer (XRD, PANalytical X'Pert PRO) with Cu radiation $\text{K}\alpha_1$ at room temperature. The dielectric properties were measured using LCR meters (HP4194A and TH2816A). Commercial temperature chambers (MPC-2000A, -65 to 150°C ; Nabertherm, 25 – 1300°C) were used to support the dielectric measurement at various temperatures.

Peer review under responsibility of The Ceramic Society of Japan and the Korean Ceramic Society.



Production and hosting by Elsevier

2187-0764 Production and hosting by Elsevier B.V. on behalf of The Ceramic Society of Japan and the Korean Ceramic Society.
<http://dx.doi.org/10.1016/j.jascers.2013.12.006>

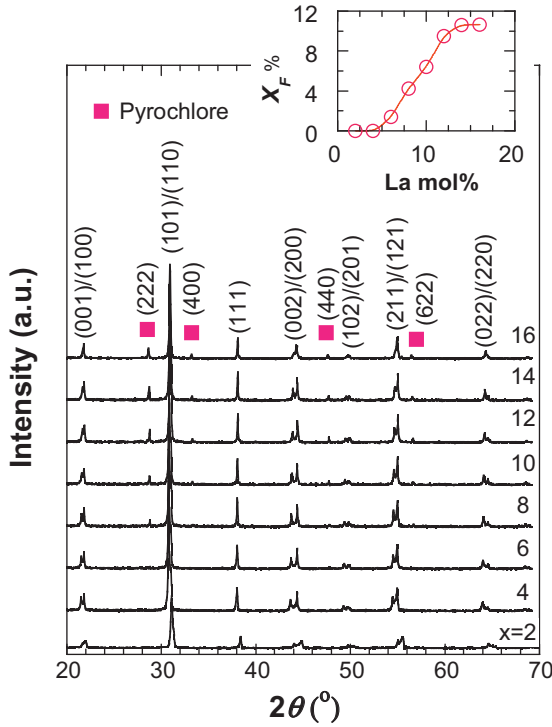


Fig. 1. XRD patterns of Sb doped PLZT $x/52/48$ ($2 \leq x \leq 16$) ceramics. Inset is the pyrochlore phase volume percentage (X_F) as a function of La concentration.

3. Results and discussion

Fig. 1 shows the XRD patterns of Sb doped PLZT ceramic powders. XRD data reveals that the Sb doped PLZT ceramics were well crystallized. For $x \leq 4$ mol%, only perovskite phase (Pe-phase) can be observed within the detection limit of XRD. For $x \geq 6$ mol%, pyrochlore phase (JCPDS 72-2370, Py-phase) was present, whose peak intensities increase with the increase of La concentration. To estimate the volume percent (X_F) of Py-phase by the ratio of the highest peak intensities, peak (222) for the Py-phase to the sum of peak (222) for the Py-phase and peak (101)/(110) for the Pe-phase, it is found that the X_F increases linearly from 0% to 10.6% in the range of $x = 5$ –14%, and are stabilized at 10.6% at $x = 16$ (the inset in Fig. 1). Based on the facts that second phase is absent in PLZT $x/52/48$ ($0 \leq x \leq 20$) [1,2,11] and the solubility limit of Sb in PZT is around 2% [12], one can expect that the Py-phase is introduced by the Sb dopants. Yet, due to the complication of the pyrochlore system ($A_2B_2O_{7-\delta}$, $A = \text{La, Sb, Pb}$, $B = \text{Zr, Ti, Sb}$) in PZT-based ceramics, the accurate chemical composition of the Py-phase is not identified. The Py-phase lattice parameters based on peak (222) are calculated as 10.67 ± 0.17 Å, suggesting a single composition in the samples. The influence of the Py-phase on the dielectric behavior is discussed as follows.

Fig. 2a shows the variation of permittivity (ϵ_r) and dielectric loss ($\tan \delta$) of Sb doped PLZT ceramics with frequency at room temperature. The values of ϵ_r and $\tan \delta$ are between 2200 and 3800, and from ~ 0.02 to 0.04, respectively. They are very much comparable to those of PLZT ceramics at the same La doping level. Generally, Py-phase is supposed to be deleterious in ferroelectric materials because of its low permittivity [13–16]. Even a small amount of Py-phase can diminish the dielectric properties intensively [3,17]. However, the samples in this study do not show such low ϵ_r values. Similar phenomena were seen in the literature [9,18], where one paper attributed it to a single phase of perovskite structure yet

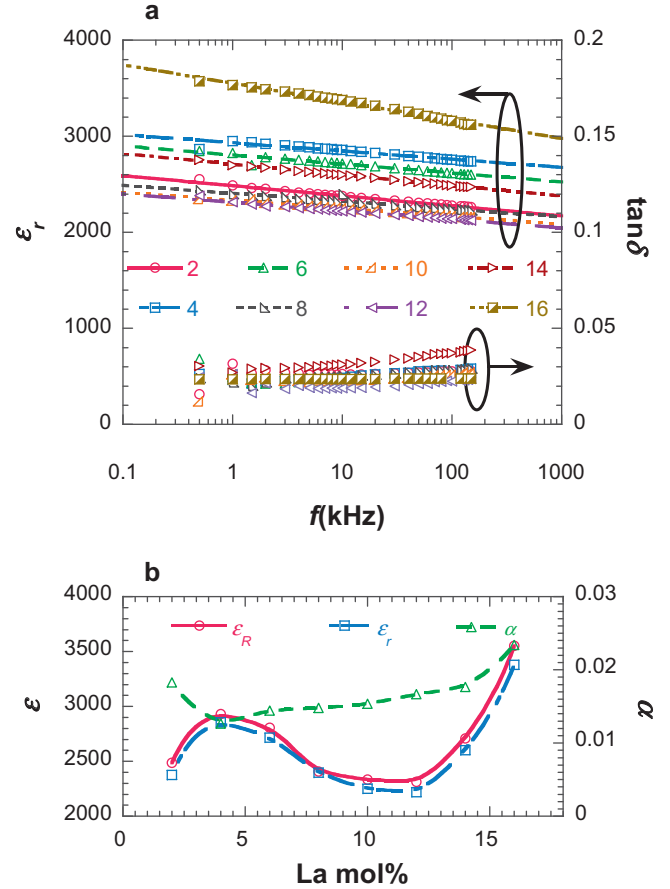


Fig. 2. (a) Room temperature permittivity (ϵ_r) and dielectric loss ($\tan \delta$) of Sb doped PLZT ($x/52/48$) as a function of frequency and (b) dependence of ϵ_r (at 1 kHz) and calculated Rayleigh law fitting parameters (ϵ_R , α) on La concentration.

with dissimilar distortion. Yamamura et al. [19] reported that such defect Py-phase compositions can have permittivity up to 10^5 – 10^7 . Thus, one of the following scenarios may occur in our samples: (a) the Py-phase is a Pe-phase in a different structure; (b) the Py-phase has comparable ϵ_r with that of Pe-phase; (c) the Py-phase has a discontinuous distribution, e.g. in the form of columns that parallel to the external electric field. Any of the above assumption can zero or minimize the influence from the Py-phase to the dielectric properties.

The dielectric behavior of ferroelectric materials adheres to Rayleigh model up to electric field of $\sim 1/2$ of the coercive electric field [20]. Note that the non-ferroelectric materials, e.g. Py-phase, do not obey the model. In a random system, where restoring forces are in normal distribution, such extrinsic contributions, e.g. domain wall motion, obey the following equation before the Debye relaxation [21–23]:

$$\epsilon(f) = \epsilon_R(1 + \alpha \lg(f)) \quad (1)$$

where f is the measure frequency, ϵ_R is the reversible permittivity, and α is the Rayleigh fitting coefficient. The frequency dependent permittivity of the samples was plotted in Fig. 2a with satisfied fitting based on Eq. (1). The fitting parameters were plotted in Fig. 2b. It is found that the reversible permittivity has very close values to those measured at 1 kHz. The Rayleigh fitting coefficients gradually increase from 0.015 to 0.025 for $4 \leq x \leq 16$, indicating the reversible domain wall motion has greater contribution to the ϵ_r at higher La concentration. Narayanan et al. [24] found that the intrinsic permittivity of PLZTs is very comparable to that of PZTs. In other words, the

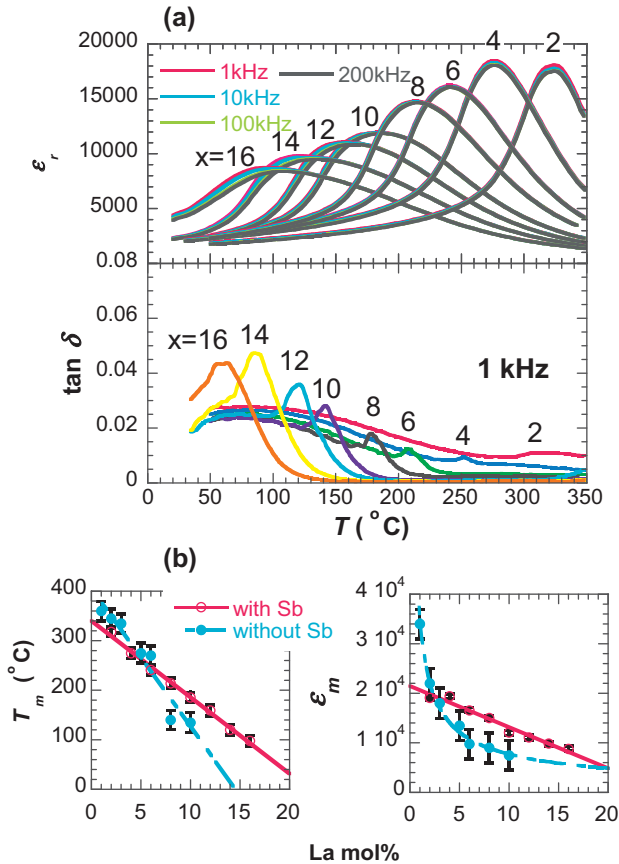


Fig. 3. (a) Temperature dependent ϵ_r and $\tan \delta$ of Sb doped PLZT ($x/52/48$) ceramics and (b) peak temperature (T_m) and peak permittivity (ϵ_m) vs. La mole fraction. Note that the PLZT data are based on compositions of $x/53/47$ adopted from Ref. [26–28].

increased permittivity at high La concentration is extrinsic due to the increase of domain wall mobility. These simulation results are expected during a typical ferroelectric-to-relaxor crossover where decreased grain/domain size eases the domain wall motion and facilitates the domain reorientation. The frequency dependence in this study, however, is weaker compared with pure PLZT. Pérez-Delfín et al. [10] reported that the ϵ_r decrease from 4000 at 0.5 Hz to 2700 at 1 MHz, leaving the value of $\alpha \approx 0.070$. But the value drops to ~ 0.010 in the same PLZT composition when MnO_2 dopant (2 wt%) are used. As Ahart et al. [25] and Pérez-Delfín et al. [10] discussed, the PNRs in relaxors can be easily aligned and grow with external electric field, but when additional dopants, e.g. Sb^{5+} , Mn^{4+} , are introduced to the system, these new cations/vacancies yield additional internal electric fields that may pin and couple to the PNRs, and break short coherent length (SCL) cation order. As a consequence, the PNRs become macro-size domains, and relaxor state disappears. Therefore, PLZT with Sb dopant is less disordered. Since non-ferroelectric compositions do not obey the Rayleigh model, the frequency dependent dielectric responses also suggested that the Py-phase has minor to no influence in the dielectric response of Sb doped PLZT.

The dielectric response for Sb doped PLZT $x/52/48$ ($2 \leq x \leq 16$) compositions is shown in Fig. 3a. The permittivity peak (ϵ_m) and temperatures (T_m) linearly decreases associating the broader permittivity peaks as the value of x increases. Dielectric frequency dispersion (frequency dependent peak drifting) is not obvious until the mole fraction of La^{3+} is higher than 10%. Similar tendency were seen in undoped PLZTs [4,6], meaning that La ions gradually transform the PZTs from ferroelectric to relaxor. The dielectric loss peaks

appeared at lower temperatures of $\sim 40^\circ\text{C}$ compared with their T_m counterparts, and then reduced to lower values at higher temperature in the paraelectric phase when domain wall vanishes. The dielectric peaks showed intense peaks in the mole fraction of La^{3+} from 10% to 16%. Such phenomenon may have strong correlation with the impurity. Yet in the form of ceramics whose dielectric loss is extrinsic, the complexity of dielectric loss can be determined by, not only the material composition, but also the metal and oxygen vacancies, local composition fluctuations, etc. Thus, more discussion on the dielectric loss is not given in this work. It has been reported that such frequency dispersion is initialized at $\text{La} = 6$ and 12 mol% in PLZT compositions of $x/65/35$ and $x/60/40$, respectively [29,30]. Thus, the ferroelectric–relaxor boundary of $\text{La} = 10$ mol%, when frequency dispersion in the samples are noticeable, is a realistic value in consideration the phase diagram of PLZTs. More detailed comparisons of the phase transition parameters T_m and ϵ_m of this study and PLZTs are illustrated in Fig. 3b. Both Sb doped PLZTs and non-doped PLZT have decreasing peak temperatures as a function of La concentration. The Sb doped PLZTs has smaller T_m and ϵ_m at low concentrations ($x \leq 4$) and greater ones at high concentrations ($x \geq 6$). The Sb dopant may generate more Pb vacancies that lower the values of T_m and ϵ_m when PLZTs are in the ferroelectric state. At higher mole fraction of La^{3+} , Sb dopant may delay and hinder the formation of PNRs. Consequently, higher values of T_m and ϵ_m were found compared with those of undoped PLZTs. To further investigate the La concentration effect in the ferroelectric–relaxor transition, and to describe qualitatively the shape of dielectric anomaly, Curie–Weiss (C–W) type law of relaxor is used to simulate the deviation from C–W law.

Two main features of $\epsilon_r(T)$ were used to identify a relaxor from a ferroelectric: (a) the broad permittivity peak (strong deviation from C–W law), namely the diffuse phase transition; (b) the frequency dispersion. The first one is usually measured with the C–W type law at $T_m \leq T \leq T_d$ (Burns temperature, above which relaxors are in paraelectric phase) [4–6]:

$$\frac{\epsilon_m}{\epsilon_r} - 1 = \frac{(T - T_m)^2}{2\delta_m^2} \quad (2)$$

where δ_m is a constant, measuring the degree of the peak diffuseness. The fitting of the data was plotted in Fig. 4a. The fitting parameter δ_m is shown in Fig. 4b, where greater values of δ_m were found in higher La concentration samples, inferring broadened peaks and the intense composition fluctuations.

One of the methods to qualitatively demonstrate the frequency dispersion is using the peak temperature drift (ΔT_m) of permittivity peaks measured at two different frequencies. The ΔT_m , defined as the value differences between T_m measured at $f = 1$ and 200 kHz, was shown in Fig. 4b. Like the trend of δ_m , the values of ΔT_m were greater at higher La concentration from 1 K at $x = 6$, to the maximum of 24 K at $x = 14$.

The frequency dispersion of Sb doped PLZTs is significant at $x \geq 14$, where dipole glass model is widely used to demonstrate the relaxor state [5,6,20]. This model adopted Vogel–Fulcher (V–F) analysis describes the freezing of the dipoles results from cooperative interactions between moments on the nanometer scale. The V–F function is given below as [5,6]:

$$f = f_0 \exp \left[\frac{-U}{k_B(T_m - T_f)} \right] \quad (3)$$

where f is the measure frequency, f_0 is a fitting coefficient related to dipole freezing time, U is the activation energy, k_B is the Boltzmann constant, and T_f is the glass freezing temperature. The fitting of the data as shown in inset of Fig. 4b yields $f_0 = 3.9 \times 10^{13}$ Hz (1.51×10^{13} Hz), $U = 0.26$ eV (0.21 eV), and $T_f = 29.0^\circ\text{C}$ (1.5°C) for

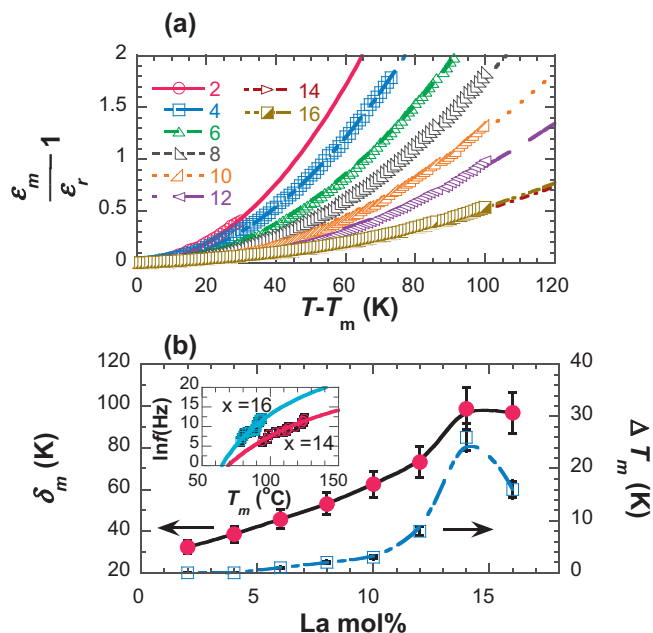


Fig. 4. (a) C–W type law fitting of diffuse phase transition above T_m and (b) as-calculated diffuse coefficients δ_m and ΔT_m vs. La concentration; Inset is the V–F law fittings for PLZT $x/52/48$ ($x = 14, 16$).

$x = 14$ mol% (16 mol%). These values are comparable to the open literature of relaxor PLZTs [31–33]. The above simulation indicates that, although Sb dopants can weaken the effects of La ions in ferroelectric–relaxor transition, at high La concentrations, 1.5 wt% Sb_2O_5 doped PLZTs can be fully transformed into relaxor state similar to non-doped PLZTs.

4. Conclusion

In conclusion, we have investigated the Sb doping and La substitution influence to the ferroelectric-to-relaxor crossover in Sb doped PLZT ceramics. The prepared samples transform from ferroelectric to relaxor as the La concentration gradually increased from 2 to 16 mol%, with a boundary at $x = 10$. La substitution eases the reversible movement of domain walls, and Sb dopants weaken such effect. Although Sb dopant weakens the formation of PNRs, Sb doped PLZTs are in pure relaxor state at high La concentration ($x \geq 14$). Our results suggest that modified relaxors with improved dielectric properties while retaining their features as relaxors can be achieved by doping in pure relaxor composition, e.g. high La concentration PLZT and $Pb(Mg_{1/3}Nb_{2/3})O_3$.

Conflict of interest statement

The authors declare that there are no conflicts of interest.

Acknowledgments

This work was supported by Fair of Science and Technical Achievements Resulted from Cooperation of Industry, Education and Academy, Guangdong, China (2010A09020059).

References

[1] G.H. Haertling and C.E. Land, *J. Am. Ceram. Soc.*, **54**, 1–11 (1971).
[2] G.H. Haertling, *J. Am. Ceram. Soc.*, **54**, 303–309 (1971).

[3] G.H. Haertling, *J. Am. Ceram. Soc.*, **82**, 797–818 (1999).
[4] L.E. Cross, in *Piezoelectricity*, Ed. by W. Heywang, K. Lubitz and W. Wrsing, Springer, Berlin, Heidelberg (2008) pp. 131–155.
[5] A.A. Bokov and Z.G. Ye, *J. Mater. Sci.*, **41**, 31–52 (2006).
[6] Z.G. Ye, *Key Eng. Mater.*, **155–156**, 81–122 (1998).
[7] S. Tong, B. Ma, M. Narayanan, S. Liu, R. Koritala, U. Balachandran and D. Shi, *ACS Appl. Mater. Interfaces*, **5**, 1473–1480 (2013).
[8] G. Heike and K. Lubitz, in *Piezoelectricity*, Ed. by W. Heywang, K. Lubitz and W. Wrsing, Springer, Berlin, Heidelberg (2008) pp. 89–130.
[9] R. Rai and S. Sharma, *Ceram. Int.*, **30**, 1295–1299 (2004).
[10] E. Pérez-Delfín, J.E. García, A. Vega-García, F. Guerrero and J.A. Eiras, *J. Eur. Ceram. Soc.*, **32**, 1659–1665 (2012).
[11] W.A. Schulze, T.G. Miller and J.V. Biggers, *J. Am. Ceram. Soc.*, **58**, 21–23 (1975).
[12] Z. Ling, W. Qiu and K. Wang, *Electro. Comp. Mater.*, **24**, 31–34 (2005).
[13] J.C. Champarnaud-Mesjard, M. Manier, B. Frit and A. Tairi, *J. Alloys Compd.*, **188**, 174–178 (1992).
[14] D. Dhak, P. Dhak and P. Pramanik, *Appl. Surf. Sci.*, **254**, 3078–3092 (2008).
[15] H. Du, H. Wang and X. Yao, *Ceram. Int.*, **30**, 1383–1387 (2004).
[16] L. Cai and J.C. Nino, *J. Eur. Ceram. Soc.*, **27**, 3971–3976 (2007).
[17] M.A. Mohiddon, R. Kumar, P. Goel and K.L. Yadav, *IEEE Trans. Dielectr. Electr. Insul.*, **14**, 204–209 (2007).
[18] S. Dutta, R.N.P. Choudhary and P.K. Sinha, *J. Alloys Compd.*, **426**, 345–351 (2006).
[19] H. Yamamura, H. Nishino and K. Kakinuma, *J. Phys. Chem. Solids*, **69**, 1711–1717 (2008).
[20] P. Bintachitt, S. Jesse, D. Damjanovic, Y. Han, I.M. Reaney, S. Trolier-McKinstry and S.V. Kalinin, *Proc. Natl. Acad. Sci. U.S.A.*, **107**, 7219–7224 (2010).
[21] D.A. Hall, *J. Mater. Sci.*, **36**, 4575–4601 (2001).
[22] F. Griggio, S. Jesse, A. Kumar, O. Ovchinnikov, H. Kim, T.N. Jackson, D. Damjanovic, S.V. Kalinin and S. Trolier-McKinstry, *Phys. Rev. Lett.*, **108**, 157604 (2012).
[23] M. Narayanan, U. Balachandran, S. Stoupin, B. Ma, S. Tong, S. Chao and S. Liu, *J. Phys. D*, **45**, 335401 (2012).
[24] M. Narayanan, S. Tong, S. Liu, B. Ma and U. Balachandran, *Appl. Phys. Lett.*, **102**, 062906 (2013).
[25] M. Ahart, M. Somayazulu, R. Cohen, P. Ganesh, P. Dera, H. Mao, R.J. Hemley, Y. Ren, P. Liemann and Z. Wu, *Nature*, **451**, 545–548 (2008).
[26] S.M. Gupta, J.F. Li and D. Viehland, *J. Am. Ceram. Soc.*, **81**, 557–564 (1998).
[27] K. Wojcik, J. Błaszczyk and J. Handerek, *Ferroelectrics*, **70**, 39–46 (1986).
[28] A. Peláiz Barranco, F. Calderón Piñar and O. Pérez Martínez, *Phys. Stat. Sol. B*, **220**, 591–595 (2000).
[29] G.A. Samara, *J. Phys. Condens. Matter*, **15**, R367–R411 (2003).
[30] G.A. Samara and E.L. Venturini, *Phase Transitions*, **79**, 21–40 (2006).
[31] J.L. Dellis, *J. Phys. Condens. Matter*, **8**, 7957–7965 (1996).
[32] S. Kamba, V. Bovtun, J. Petzelt, I. Rychetsky, R. Mizasas, A. Brilingas, J. Banys, J. Grigas and M. Kosec, *J. Phys. Condens. Matter*, **12**, 497–519 (2000).
[33] F. Cordero, F. Craciun, A. Franco, D. Piazza and C. Galassi, *Phys. Rev. Lett.*, **93**, 097601 (2004).

Sheng Tong*
Zhiyuan Ling**

Department of Electronic Materials Science and Engineering, School of Materials Science and Engineering, South China University of Technology, Guangzhou 510640, China

* Corresponding author. Current address: Nanoscience and Technology Division, Argonne National Laboratory, Argonne, IL 60439, USA. Tel.: +1 630252 4628; fax: +1 630252 4646.

** Corresponding author. E-mail addresses: stong@anl.gov, shengtong@mail.uc.edu (S. Tong), imzyling@scut.edu.cn (Z. Ling)

30 November 2013

22 December 2013

27 December 2013

Available online 19 January 2014